Variations in the surface structure and composition of tungsten oxynitride catalyst caused by exposure to air

Deug-Hee Cho [a], Tae-Sun Chang [a] and Chae-Ho Shin [b,*]

[a] *Advanced Chemical Technology Division, Korea Research Institute of Chemical Technology, PO Box 107, Yusong, Taejon 305-343, Korea*
[b] *Department of Chemical Engineering, Chungbuk National University, Cheongju, Chungbuk 361-763, Korea*
E-mail: chshin@cbucc.chungbuk.ac.kr

Received 15 January 2000; accepted 11 April 2000

A tungsten oxynitride ($WN_{0.59}O_{0.24}$) catalyst with a specific surface area of 63.7 $m^2\,g^{-1}$ has been prepared by the temperature-programmed reaction of WO_3 with NH_3 and characterized by elemental analysis, X-ray powder diffraction, N_2 sorption, and X-ray photoelectron spectroscopy (XPS) in order to extensively investigate the textural variation of this material caused by exposure to ambient air. No noticeable changes in the bulk structure of tungsten oxynitride prepared here are caused by the sample storage in ambient conditions for a long period of time up to 80 days. However, its N_2 BET surface area and total pore volume were found to severely decrease with increasing the period of time of exposure to air. The XPS depth profile measurements reveal that the amorphous tungsten trioxide (WO_3) species is formed on the surface of tungsten oxynitride upon exposure to air, which results in the significant modification of the surface structure and composition of the oxynitride material. In contrast, no indications of other surface tungsten phases such as dioxidic, monooxidic, and oxynitridic species are detected. The overall results of this study strongly suggest that oxygen is mobile enough to diffuse into the surface or near-surface of the oxynitride lattice even in ambient conditions, leading to the surface WO_3 formation.

Keywords: tungsten oxynitride, tungsten suboxides, XPS depth profile, N_2 sorption

1. Introduction

Since the pioneering work of Boudart in the early 1970s, the use of transition metal carbides and nitrides for heterogeneous catalysis has been the subject of a wide variety of experimental and theoretical investigations [1–5]. It is now well-established that these new classes of catalytic materials behave like the noble group metals for many hydrogen transfer reactions such as ammonia synthesis [6], methane production from CO and CO_2 [3,7], ethylene hydrogenation [3,8], and butane hydrogenolysis [9]. In addition, they are known to exhibit excellent hydrodenitrogenation (HDN) and hydrodesulfurization (HDS) activities in the treatment of coal-derived liquids; in particular, molybdenum carbide and nitride, both supported and unsupported, are more active than a commercial sulfided Ni–Mo/Al_2O_3 catalyst in quinoline HDN [10].

It has been repeatedly shown that the catalytic properties of transition metal carbides and nitrides can be greatly affected by the manner in which they are kept or activated prior to use as catalysts [11]. For example, oxidative treatment of carbides of molybdenum and tungsten at elevated temperatures gives catalysts capable of alkane isomerization without extensive hydrogenolysis that is commonly observed for clean carbide surfaces [12,13]. The origin of isomerization activity has been attributed to the formation of new catalytically active phases, i.e., surface oxycarbides, during the oxygen pretreatment step. Apparently, the phenomenon of heterogeneous catalysis is governed by the surface and/or near-surface properties of the solid catalysts employed. Thus, the presence of superficial oxygen atoms on carbides or nitrides can modify the physicochemical and catalytic properties of the resulting materials in a significantly different manner than those of the pure carbide or nitride phases.

Transition metal oxycarbides and oxynitrides are commonly found as intermediates, in some cases as final products, during the synthesis of the corresponding metal carbides and nitrides [14–17]. For example, Lucy et al. have synthesized several tungsten oxynitride materials using the temperature-programmed reaction of tungsten trioxide with ammonia [18]. As described above, in addition, thermal treatment of pure carbides and nitrides in an oxidizing atmosphere or even exposure to ambient air is reported to result in the formation of such non-stoichiometric, oxygen-containing materials. Here we present the results obtained from powder X-ray diffraction, elemental analysis, nitrogen adsorption, and X-ray photoelectron spectroscopic measurements of a series of tungsten oxynitrides exposed to air at room temperature for different periods of time in order to explore the effects of chemisorbed oxygen on the surface structure and composition of the as-prepared tungsten oxynitride catalyst. There are many investigations on changes in the textural properties of pure carbides or nitrides caused by oxygen pretreatment. However, few studies have thus far focused on the characterization of the oxygen-treated oxycarbides or oxynitrides.

* To whom correspondence should be addressed.

2. Experimental

A tungsten oxynitride with a N_2 BET surface area of 63.7 $m^2\,g^{-1}$ was prepared by the temperature-programmed reaction of WO_3 (99.99%, Aldrich) with ammonia (99.99%, Matheson), following a modification of the procedures developed by Volpe and Boudart [2,19]. WO_3 powder was used without further pretreatment. NH_3 was purified using a KOH trap to remove residual water and then fed into a tubular quartz reactor (18 mm o.d.) containing 1.0 g of WO_3 powder at a flow rate of 47.1 μmol s^{-1} using a Matheson 8274 mass flow controller. The nitridation temperature was first increased from room temperature to 473 K at a rate of 0.028 K s^{-1}, and then to the final temperature (923 K) at a heating rate of 0.008 K s^{-1}. After holding at the same temperature for 2 h, the nitrided sample was purged with He there for 1 h to remove residual NH_3. Finally, the sample was passivated with 1% O_2 in He at room temperature for 1 h at a flow rate of 49.6 μmol s^{-1} to avoid further reoxidation. The temperature control of all procedures given above was carried out using a Hanyoung P-100 temperature programmer with a type K thermocouple that was placed on the powder bed. The evolution of NH_3 decomposition with time on stream during the temperature-programmed WO_3 nitridation was monitored on-line by a Chrompack CP 9001 gas chromatograph equipped with a thermal conductivity detector, and a Chromosorb 103 column was used in order to separate NH_3, H_2, and H_2O. The line of effluent gases was heated at 393 K to prevent the condensation of H_2O vapor, and the analysis was performed every 20 min using N_2 as a carrier gas. Thus, the measurement for the amount of N_2 produced during the decomposition of NH_3 was not attempted here. The tungsten oxynitride synthesized by the procedures described above was stored under ambient air for a given period of time up to 80 days.

The bulk structure and crystallinity of all solids studied here were determined by powder X-ray diffraction (XRD) using a Rigaku D/Max-IIA diffractometer (Cu K_α radiation). The unit cell parameters of the face-centered cubic tungsten oxynitride phases were determined by indexing the XRD patterns recorded with Si powder as an internal standard and then refined using a least-squares procedure. Chemical analysis was performed by a CEC 240-XA elemental analyzer. Before starting chemical analysis for O and N, the samples were outgassed in a vacuum of 10^{-3} Torr at 523 K for 2 h. The W content of the as-prepared oxynitride sample was calculated from the observed difference in the masses of WO_3 and oxynitride phases, by assuming that there is no W loss during the temperature-programmed nitridation step. The BET surface area and total pore volume measurements were carried out by the nitrogen adsorption at 77 K with a volumetric method using a Micromeritics ASAP 2405 analyzer. The method of Barrett, Joyner, and Halenda (BJH) was used to determine the pore size distribution of the samples. X-ray photoelectron spectroscopic (XPS) measurements were performed on a VG Scientific ESCALAB 210 spectrometer with a Mg K_α X-ray source (1253.6 eV). The pressure inside the analysis chamber was typically maintained at better than 5×10^{-10} Torr. The XPS spectra were recorded during sputtering with 3.0 keV Ar^+ ions in order to obtain the depth profile of the air-exposed tungsten oxynitride sample. All the binding energies are referenced to the C 1s line at 284.6 eV from adventitious carbon. The binding energy values reported here are within an accuracy of $\pm$0.3 eV. The W 4f spectra obtained were deconvoluted using the peak fit curve-fitting software. Their spectral deconvolution was constrained so that the multiplicity factor between the W $4f_{5/2}$ and $4f_{7/2}$ core levels and their splitting (ΔW 4f) are 6/8 and 2.1 $\pm$ 0.2 eV, respectively. The relative ratios of W species in the oxynitride surface were estimated on the basis of comparisons of the integrated W 4f XPS band intensities by assuming that all the W species have the same relative sensitivity factor. The band intensities were evaluated by using the straight-line background method.

3. Results and discussion

3.1. Synthesis of tunsgten oxynitride

Figure 1 shows changes with time on stream in the production of H_2O and H_2, as well as in the decomposition of NH_3, during the temperature-programmed reduction and nitridation of WO_3. It can be seen that H_2O begins to be produced at temperatures higher than 683 K. This implies that WO_3 is reduced to its suboxides at $T \geqslant 683$ K, since H_2O production is a result of WO_3 reduction with H_2 produced by NH_3 decomposition. As illustrated in figure 1, in addition, the H_2O production profile is characterized by two peaks which appear in the temperature regions of 800–820 and 900–920 K. We note here that the nitridation of

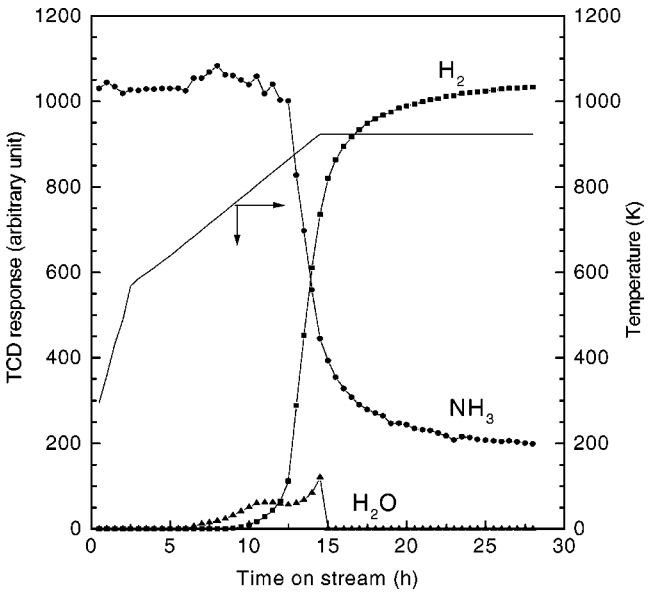

Figure 1. Dependence of the decomposition of NH_3 and the production of H_2 and water on the time on stream during the reduction–nitridation step of the precursor WO_3.

WO_2 under the conditions described above yields only one H_2O production peak at 900–920 K. Therefore, it appears that the low- and high-temperature H_2O production peaks observed in figure 1 may be due to the formation of at least two different suboxides, most likely WO_2 and WO phases, respectively. On the other hand, the H_2 production caused by NH_3 decomposition begins to be detected at $T \geqslant 783$ K, a 100 K shift upward when compared to the temperature for the first production of H_2O. This can be rationalized by suggesting that most, if not all, of the H_2 molecules produced at the beginning of the nitridation of WO_3 are preferentially consumed by the oxide reduction to form H_2O, which may result in the shift of detection temperature for the initial formation of H_2O to a higher temperature region. Figure 1 also shows that upon further elevating the nitridation temperature to 923 K, the H_2 production increases very sharply, while the opposite is observed for the outlet concentration of NH_3. In contrast, the isothermal nitridation of WO_3 at 923 K for 10 h time on stream gives a slight increase in the H_2 production with no noticeable H_2O production. Therefore, it is most likely that the extent of WO_3 nitridation almost reaches its maximum during the first few hours of the isothermal treatment at 923 K. This has been further ascertained by XRD experiments and led us to select the sample nitrided at the final temperature for 2 h and subsequently passivated with 1% O_2 in He at room temperature for 1 h, as a reference material in an attempt to explore the effects of chemisorbed oxygen on the textural properties of tungsten oxynitride catalyst.

3.2. XRD analysis

Figure 2 shows the XRD patterns of a series of tungsten oxynitrides exposed to air as a function of time up to 80 days. The XRD pattern in figure 2(a) was obtained from as-passivated oxynitride and shows the typical features of β-W_2N with a face-centered cubic lattice. Also, no indications of impurity phases are detected. Chemical analysis reveals that the oxynitride sample prepared in this study has an overall composition of $WN_{0.59}O_{0.24}$, within experimental error. Thus, the nitrogen content of this oxynitride sample was found to be smaller than that of stoichiometric WN but larger than that of W_2N. A similar result has been reported for other oxynitride materials like molybdenum oxynitrides and tugsten oxynitrides [18,21]. When the complete XRD pattern of the as-passivated oxynitride was indexed on the basis of a cubic cell, its unit cell parameter was calculated to be 4.157 Å which is slightly larger than that (4.126 Å) of β-W_2N [18,20]. This is not unexpected because the nitrogen content of oxynitride prepared here is higher than that of β-W_2N. As shown in parts (b)–(d) of figure 2, on the other hand, no reflections other than those from tungsten oxynitride are observed even from the sample exposed to air for 80 days. Also, no significant changes in the position and intensity of the X-ray peaks for the as-passivated oxynitride are detected. This clearly shows that the bulk structure of this material is not affected by exposure to air.

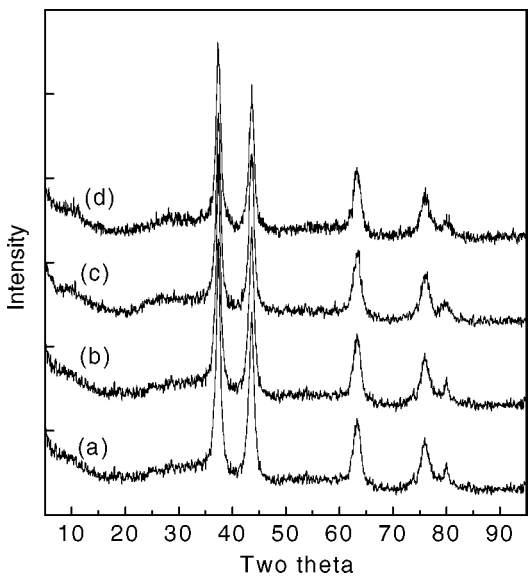

Figure 2. X-ray diffraction patterns of a series of tungsten oxynitrides exposed to ambient air for different periods of time: (a) 0, (b) 20, (c) 40, and (d) 80 days.

3.3. Nitrogen sorption measurements

Figure 3 shows the N_2 sorption isotherms of tungsten oxynitrides exposed to air for different periods of time. The isotherm of the material treated under flowing H_2 at 773 K for 4 h after exposure to air for 80 days is also given in figure 3. All the isotherms of materials studied here are characterized by the typical type IV mesopore sorption behavior, with the initial steep increase in sorption, inflection at about $P/P_0 = 0.5$, and saturation of the mesopores at

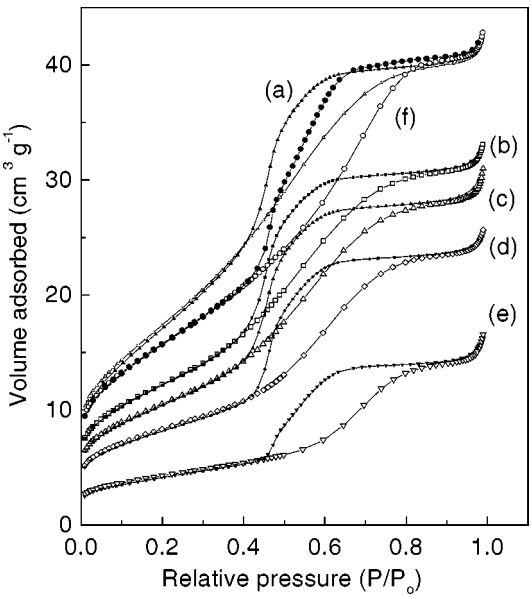

Figure 3. N_2 sorption isotherms of tungsten oxynitrides before and after exposure to air at room temperature: (a) as-passivated, exposed to ambient air for (b) 10, (c) 20, (d) 40, (e) 80 days, and (f) subsequently treated under flowing H_2 at 773 K for 4 h. Open and closed symbols represent adsorption and desorption, respectively.

Table 1
Changes in the N_2 BET surface area and total pore volume of tungsten oxynitride as a function of the period of time of exposure to air.

Period of exposure time to air (days)	S_{BET} ($m^2\,g^{-1}$)	Total pore volume ($cm^3\,g^{-1}$)
0	63.7	0.065
10	44.1	0.050
20	38.0	0.046
40	30.0	0.039
80	15.3	0.026
80[a]	57.1	0.066

[a] Followed by H_2 treatment at 773 K for 4 h.

about $P/P_0 = 0.6$. In addition, the presence of hysteresis in their desorption branches clearly shows that they have interparticular mesoporosity. The BET surface areas and total pore volumes of a series of oxynitride materials studied here were calculated from their N_2 adsorption isotherms and are listed in table 1. The fact that the as-passivated oxynitride has a surface area of 63.7 $m^2\,g^{-1}$ indicates that the formation of the high surface area tungsten oxynitride can be achieved by the nitridation of WO_3 with a low surface area (1.0 $m^2\,g^{-1}$) in a temperature-programmed method, revealing the pseudomorphic nature of the reaction which has been repeatedly shown in a number of previous studies [2,18,19]. Another important observation is that the surface area of tungsten oxynitride prepared here severely decreases with increasing time on exposure to air. For example, the BET surface area (15.3 $m^2\,g^{-1}$) of the material exposed to air for 80 days was found to be only one fourth as compared to that of as-passivated oxynitride. The same trend was also observed from the total pore volumes given in table 1. These results are in qualitative agreement with those reported by Lucy et al. [18]. It is well-established that the passivation of transition metal nitrides or oxynitrides in an oxidizing atmosphere causes the formation of a thin oxide layer on their surface and thus leads to lower surface area materials [21]. Therefore, a continuous loss in surface area of tungsten oxynitride with increasing time exposure to air can be explained by suggesting that the oxynitride surface is not stable enough to avoid further oxidation even after passivation. This taken on in total leads us to believe that the formation of WO_3 species continues to occur on the tungsten oxynitride surface, due to oxygen chemisorbed during exposure to air, as further evidenced by XPS experiments (*vide infra*). Also, it should be noted from table 1 that the surface area of oxynitride exposed to air for 80 days is restored to about 90% of the value of as-prepared material when subsequently treated with H_2 at 773 K for 4 h. This demonstrates that most, but not all, of the WO_3 formed can be removed by H_2 reduction at elevated temperatures.

Figure 4 shows the BJH pore size distribution curves calculated from the desorption branches in figure 3. The pore size distribution curve for the as-passivated tungsten oxynitride is represented by a mesopore with the BJH pore size of about 3.5 nm at the maximum of the distribution, which must be a main contribution to the total pore volume. In addition to this mesopore, however, there are two

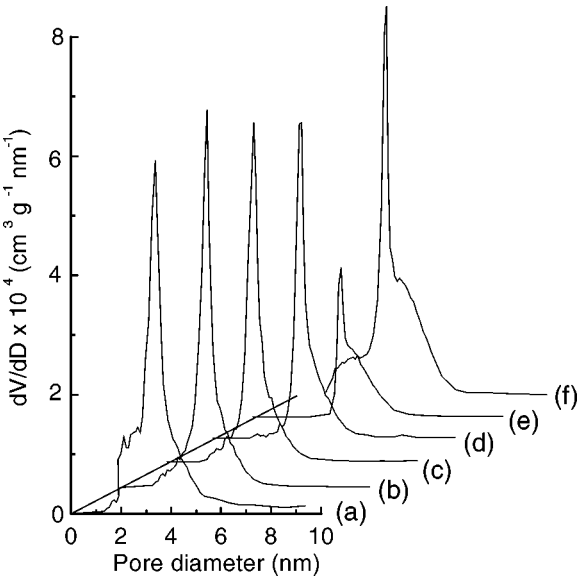

Figure 4. Barrett–Joyner–Halenda (BJH) pore size distribution curves for tungsten oxynitrides before and after exposure to air at room temperature: (a) as-passivated, exposed to air for (b) 10, (c) 20, (d) 40, (e) 80 days, and (f) subsequently treated under flowing H_2 at 773 K for 4 h.

other types of mesopores with average pore sizes of about 2.3 and 4.2 nm, as seen in figure 4(a). The existence of three types of mesopores in tungsten oxynitride prepared here can be further confirmed by the pore size distribution curve in figure 4(f), which was obtained from the material reduced with H_2 at 773 K after exposure to ambient air. Among the mesopores present in the as-passivated oxynitride, on the other hand, the 2.3 nm mesopore disappears first with increasing time on exposure to air and in turn the 3.5 nm mesopore becomes lost. As seen in curves (b)–(e) of figure 4, however, the 4.2 nm mesopore remains almost intact even after exposure to air for 80 days. In addition, no significant variations in the average pore size of the remaining mesopores are caused by exposure to air. These results strongly suggest that the formation of WO_3 in tungsten oxynitride occurs inside the smaller pores in advance of larger pores, leading to a serious pore blockage.

3.4. XPS analysis

To more accurately investigate changes in the surface properties of tungsten oxynitride caused by exposure to air, we have selected the sample stored under ambient air for 40 days and performed XPS measurements on this sample while sputtering with 3.0 kV Ar^+ ions. Figure 5 shows the representative W 4f XPS spectra of this oxynitride, measured as a function of sputtering time, together with the simulated spectra and their deconvoluted components. Table 2 summarizes the binding energies and bandwidths of the deconvoluted components of each simulated spectrum.

Figure 5(a) was obtained from the sample before Ar^+ ion sputtering. The curve deconvolution of this spectrum reveals the presence of two sets of W core levels: one is characterized by the doublet at 38.2 and 36.1 eV, while

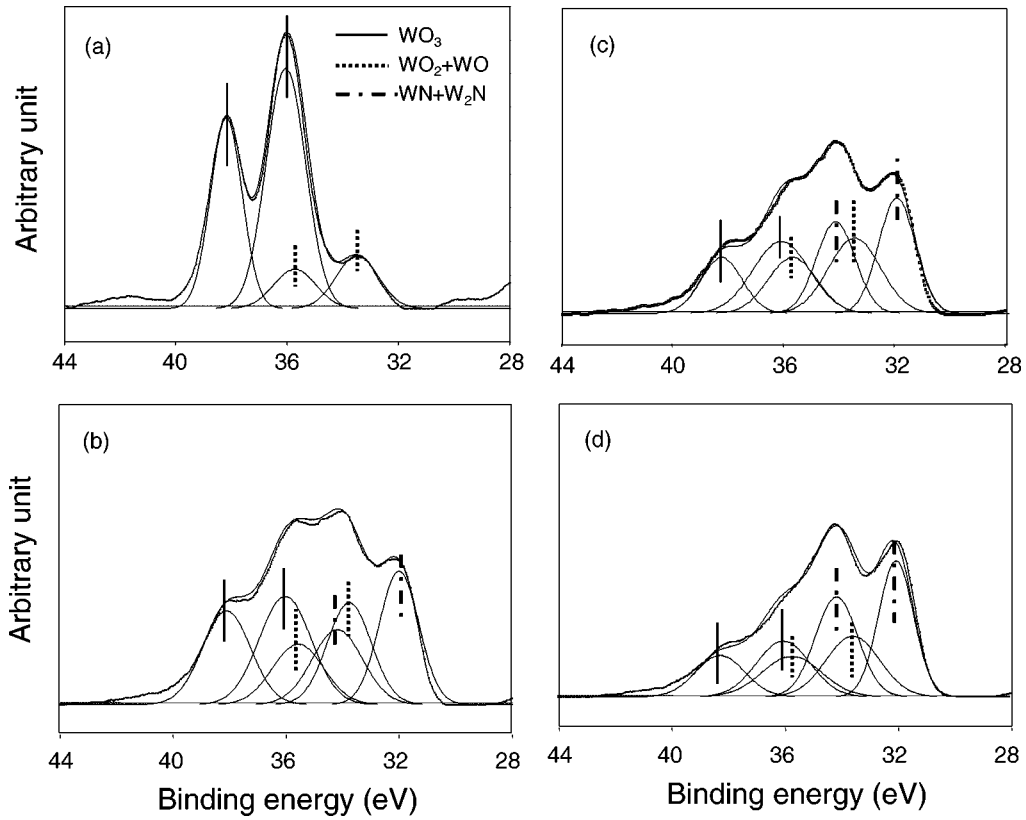

Figure 5. Curve deconvolution of selected W 4f XPS spectra recorded during sputtering with 3.0 kV Ar^+ ions of the tungsten oxynitride exposed to ambient air for 40 days. The sputtering time: (a) 0, (b) 13, (c) 25, and (d) 70 min. The dotted lines represent the experimental spectra and the solid lines are the simulated spectra. The deconvoluted components of each simulated spectrum are shown with thin solid lines.

Table 2
W 4f XPS binding energies and bandwidths of the tungsten oxynitride exposed to air for 40 days, as a function of time on Ar^+ ion sputtering.

Sputtering time (min)	Binding energies[a] (fwhm[b]) (eV)					
	WO_3		WO_2 + WO		W_2N + WN	
	W $4f_{5/2}$	W $4f_{7/2}$	W $4f_{5/2}$	W $4f_{7/2}$	W $4f_{5/2}$	W $4f_{7/2}$
0	38.2 (1.6)	36.1 (1.9)	35.7 (1.8)	33.5 (1.8)	–	–
4	38.2 (2.0)	36.1 (2.3)	35.7 (2.2)	33.5 (2.0)	34.2 (1.6)	32.0 (1.4)
13	38.2 (2.0)	36.1 (2.4)	35.6 (2.1)	33.5 (1.9)	34.2 (2.1)	32.0 (1.7)
25	38.2 (1.7)	36.1 (2.4)	35.7 (2.1)	33.5 (2.2)	34.1 (1.7)	32.0 (1.6)
44	38.1 (1.9)	36.0 (2.4)	35.8 (2.4)	33.7 (1.9)	34.1 (1.9)	32.0 (1.6)
70	38.2 (2.0)	36.0 (2.5)	35.7 (2.5)	33.6 (1.8)	34.1 (1.8)	32.0 (1.5)

[a] Binding energies are referenced to C 1s = 284.6 eV.
[b] Full width at half-maximum of the XPS band.

the other shows the doublet at 35.7 and 33.5 eV. Also, the relative intensity ratio of these two doublets was calculated to be ca. 4.3 : 1. According to the XPS data for tungsten compounds in the literature, the W $4f_{5/2}$ and $4f_{7/2}$ core levels of bulk WO_3 are reported to appear at 38.2 and 36.1 eV, respectively [22,23]. Therefore, it is most likely that the surface of the tungsten oxynitride material before Ar^+ ion sputtering is composed primarily of the trioxide species of W, i.e., WO_3. If such is the case, a continuous decrease in the S_{BET} and total pore volume of the as-passivated tungsten oxynitride caused by exposure to air for a longer period of time can be rationalized in terms of the formation of oxidic phases inside the pores. We believe that the oxidic phases formed during the exposure to air on the tungsten oxynitride prepared here may be amorphous rather than crystalline, because no reflections except those from the as-passivated oxynitride were detected by XRD (*vide ante*). On the other hand, high-resolution synchrotron XPS studies on various tungsten oxides have demonstrated that due to the lower oxidation state (4+), W in WO_2 exhibits the W $4f_{5/2}$ and $4f_{7/2}$ core levels at 35.3 and 33.2 eV that are lower by 2.9 eV than those of WO_3 [23]. In contrast, the magnitude of the W 4f core-level shift for W with formal oxidation states of 4+ and 2+ (i.e., equivalent to WO) is reported to be only 0.8 eV, which is smaller than the one third of the W 4f core-level energy difference between

WO_3 and WO_2. Also, notice that this value is smaller than half the full width at half-maximum (fwhm) of each W 4f XPS band listed in table 2. Because of its low resolution, as a direct consequence, it was not possible to further deconvolute the W 4f doublet appearing at 35.7 and 33.5 eV in figure 1(a) into the separate contributions from WO_2 and WO phases. However, the possibility that the WO species is present in tungsten oxynitride prepared here cannot be ruled out, due to the imperfect nitridation of the precursor WO_3. Therefore, we speculate that the low binding energy doublet in figure 5(a) must be attributed to the mixture of WO_2 and WO rather than WO_2 only.

Another interesting result obtained from figure 5 is that Ar^+ ion sputtering of the air-exposed oxynitride material results in the appearance of an additional W core doublet at 34.2 and 32.0 eV. This doublet becomes stronger at a longer period of sputtering time. Although few XPS studies on the pure tungsten nitride (W_2N or WN) and oxynitride materials have thus far been published, Nagai and Kishida [24] reported that a W_2N film deposited on the Si(100) wafer shows the W $4f_{5/2}$ and $4f_{7/2}$ core levels at 33.0 eV and 30.8 eV. In addition, the W 4f levels for the mixed phase of W_2N and WN were found to appear at 33.8 and 31.6 eV [25]. These studies suggest that like the case of W in W_2C and WC, the magnitude of the 4f core-level shift for W in W_2N and WN may be smaller than the fwhm values of the W 4f XPS bands. Therefore, it appears that a new doublet appearing at 34.2 and 32.0 eV in parts (b)–(d) of figure 5 must be assigned to the combination of W_2N and WN species. Further study using a high-resolution XPS excited by synchrotron radiation is necessary to separate contributions from each nitridic species. Figure 5 also shows that a decrease of the band intensity of W $4f_{5/2}$ and $4f_{7/2}$ core levels for a WO_3 phase is initially fast but slows down with sputtering time. Thus, their band intensities are still notable even after sputtering for a period of time longer than 1 h. This indicates that the surface WO_3 species cannot be completely removed by sputtering. Such a difficulty in eliminating the surface WO_3 layers has been reported for several metal carbides or nitrides. For example, Muller et al. [13] observed that the oxide layers formed on the surface of WC by adsorption of oxygen still remain even after successive catalytic experiments as in hydrocarbon reforming [13,26]. On the other hand, all the O 1s XPS spectra (not shown) of tungsten oxynitride materials before and after Ar^+ ion sputtering exhibit only one broad and symmetric band at 530.7 eV. The intensity of this band decreases continuously with increasing the period of sputtering time, which is a clear indication of the removal of the surface WO_3 species during the sputtering step. This can be further supported by the fact that a symmetric N 1s band appearing at 397.5 eV in the XPS spectrum of tungsten oxynitride material before sputtering becomes weaker with a longer period of sputtering time, but no shifts in the band position are observed.

It is well known that the XPS technique is very useful for studying the composition of a variety of solid surfaces

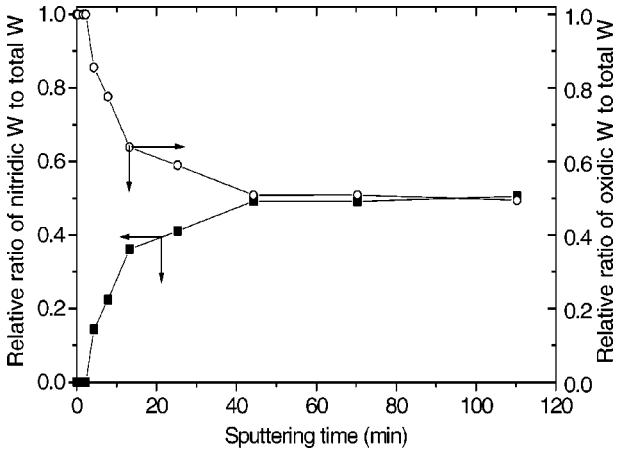

(a)

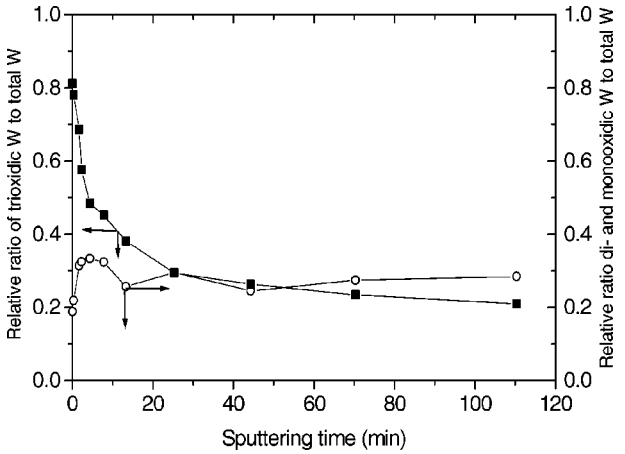

(b)

Figure 6. Plots of relative ratios of (a) nitridic and oxidic W species and (b) WO_3 and WO_2 + WO species to all the W species in the tungsten oxynitride material exposed to air for 40 days vs. sputtering time.

including transition metal carbides and nitrides [11,26–28]. As illustrated in figure 6, thus, a comparison of the intensity ratios of a specific W 4f doublet to all the W 4f doublets with respect to time on Ar^+ ion sputtering can provide some insight into the route by which the oxidic phases are formed on the oxynitride surface. Figure 6(a) shows plots of the intensities of nitridic and oxidic W 4f core levels to all the W 4f core levels (i.e., the relative ratios of nitridic and oxidic W species) versus sputtering time. To the best of our knowledge, no detailed studies on changes in the surface composition of the transition metal oxycarbide and oxynitride materials caused by exposure to air have thus far been published. In the case of transition metal carbides and nitrides, however, it has been repeatedly speculated that exposure to ambient air results in the formation of surface oxycarbides and oxynitrides with catalytic properties different from those of pure carbide or nitride phase [11,29]. Thus, if the same result is observed for the surface of oxynitride studied here, the relative ratio of nitridic W species in this material should decrease with increasing sputtering time due to the presence of surface oxynitride species. As

seen in figure 6(a), however, the relative ratio of nitridic W species increases rapidly at the early stage of sputtering, and then a rather continuous increase is observed for the period of sputtering time studied here. This clearly shows that exposure to air does not cause the formation of the surface oxynitride species. Figure 6(a) also shows that the relative ratio (0.51) of nitridic W species in the oxynitride material Ar^+ ion sputtered for 110 min is still smaller than the N/(N + O) ratio (0.71) estimated from chemical analysis. This is not unexpected because a considerable amount of WO_3 still remains on the surface even after such a long sputtering (see figure 5). On the other hand, the exact opposite is observed for changes in the relative ratio of oxidic W species. This again shows that the surface of oxynitride studied here is covered only with the oxidic W phases that are successively removed during the sputtering. To further examine which oxidic phase represents the oxynitride surface, the relative ratios of the WO_3 species and the WO_2 + WO species have been plotted with respect to sputtering time and are given in figure 6(b). As expected, the relative ratio of the WO_3 species (i.e., the trioxidic W/total W ratio) decreases continuously with increasing sputtering time. In contrast, the (dioxidic W + monooxidic W)/total W ratio increases upon increasing time on sputtering up to 5 min, reaching a value of ca. 0.3 that is almost the same as the bulk O/(N + O) ratio (0.29) obtained from chemical analysis. Then, it remains almost unchanged during the period of sputtering time studied. Therefore, it is clear that no surface tungsten species other than WO_3 are formed by exposure of the oxynitride material. This suggests that oxygen is mobile enough to diffuse into the surface or near-surface of the oxynitride lattice even in ambient conditions, leading to the formation of the surface WO_3. Finally, it has been speculated that the exposure of pure transition metal carbides or nitrides to air leads to the formation of the surface oxycarbide or oxynitride species [11,26,27]. Based on our XPS results, however, we cannot exclude the possibility that the corresponding metal oxide is the only species formed on the surface of pure carbide or nitride phase, because the oxycarbide or oxynitride is not stable in an oxidizing atmosphere.

In conclusion, the overall results of this study demonstrate that the surface of the as-passivated tungsten oxynitride is continuously transformed into tungsten trioxide (WO_3) upon exposure to ambient air, although no noticeable changes in its bulk structure are observed. However, no indications of other surface tungsten phases such as dioxidic, monooxidic, and oxynitridic species are detected. Thus, a continuous decrease in N_2 BET surface area and total pore volume with increasing the period of time of exposure to air can be attributed to the formation of the surface trioxide WO_3 species, which can modify the surface properties of the oxynitride in a significantly different manner than those of the as-passivated or as-synthesized material.

Acknowledgement

We thank Professor S.B. Hong of the Department of Chemical Technology at the Taejon National University of Technology for many helpful discussions. The financial support of this work was provided by the Chungbuk National University Development Foundation.

References

[1] R.B. Levy and M. Boudart, Science 181 (1973) 547.
[2] L. Volpe and M. Boudart, Catal. Rev. Sci. Eng. 27 (1985) 515.
[3] S.T. Oyama and G.L. Haller, Catalysis 5 (1982) 333.
[4] S.T. Oyama, in: *The Chemistry of Transition Metal Carbides and Nitrides*, ed. S.T. Oyama (Chapman & Hall, Glasgow, 1996) ch. 1.
[5] L.E. Toth, in: *Transition Metal Carbides and Nitrides* (Academic Press, New York, 1971).
[6] L. Volpe and M. Boudart, J. Phys. Chem. 90 (1986) 4874.
[7] M. Saito and R.B. Anderson, J. Catal. 63 (1980) 438.
[8] I. Kojima, E. Miyazaki, Y. Inoue and I. Yasumori, J. Catal. 73 (1982) 128.
[9] L. Leclercq, M. Provost, H. Pastor and G. Leclercq, J. Catal. 117 (1989) 384.
[10] S. Ramathan and S.T. Oyama, J. Phys. Chem. 99 (1995) 16365.
[11] G. Leclercq, M. Kamal, J.-F. Lamonier, L. Feigenbaum, P. Malfog and L. Leclercq, Appl. Catal. A 121 (1995) 169.
[12] M.J. Ledoux, C. Pham-Huu, A.P.E. York, E.A. Blekkan, P. Delporte and P. Del Gallo, in: *The Chemistry of Transition Metal Carbides and Nitrides*, ed. S.T. Oyama (Chapman & Hall, Glasgow, 1996) ch. 20.
[13] A. Muller, V. Keller, R. Ducros and G. Maire, Catal. Lett. 35 (1995) 65.
[14] C.H. Shin, G. Bugli and G. Djega-Mariadassou, J. Solid State Chem. 95 (1991) 145.
[15] H.S. Kim, C.H. Shin, G. Bugli, M. Bureau-Tardy and G. Djega-Mariadassou, Appl. Catal. A 119 (1994) 223.
[16] G. Djega-Mariadassou, C.H. Shin and G. Bugli, J. Mol. Catal. A 141 (1999) 263.
[17] C.H. Jaggers, J.N. Michaels and A.M. Stacy, Chem. Mater. 2 (1990) 150.
[18] T.E. Lucy, T.P. St. Clair and S.T. Oyama, J. Mater. Res. 13 (1998) 2321.
[19] L. Volpe and M. Boudart, J. Solid State Chem. 59 (1985) 332.
[20] JCPDS file Nos. 25-1257 and 37-571.
[21] X. Gouin, P. Marchand, P. L'Haridon and Y. Lauent, J. Solid State Chem. 109 (1994) 175.
[22] F.J. Himpsel, J.F. Morar, F.R. McFeely and R.A. Pollak, Phys. Rev. B 30 (1984) 7236.
[23] J.F. Morar, F.J. Himpsel, J.L. Hughes, J.L. Jordan, F.R. McFeely, and G. Hollinger, J. Vac. Sci. Technol. A 3 (1985) 1477.
[24] M. Nagai and K. Kishida, Appl. Surf. Sci. 70 (1993) 759.
[25] R.J. Colton and J.W. Rabalais, Inorg. Chem. 15 (1976) 236.
[26] A. Keller, M. Cheval, F. Maire, P. Wehrer, R. Ducros and G. Maire, Catal. Today 17 (1993) 493.
[27] A. Keller, M. Cheval, M. Vayer, R. Ducros and G. Maire, Catal. Lett. 10 (1991) 137.
[28] T.L. Barr, in: *Modern ESCA: The Principles and Practice of X-ray Photoelectron Spectroscopy* (CRC Press, Boca Raton, 1995).
[29] G. Djega-Mariadassou, M. Boudart, G. Bugli and C. Sayag, Catal. Lett. 31 (1995) 411.